Determination of the elastic moduli in Li Al O 2

Fabian Jachmann, M. Pattabiraman, and Carsten Hucho

Citation: Journal of Applied Physics **98**, 073501 (2005); doi: 10.1063/1.2061889
View online: http://dx.doi.org/10.1063/1.2061889
View Table of Contents: http://scitation.aip.org/content/aip/journal/jap/98/7?ver=pdfcov
Published by the AIP Publishing

Determination of the elastic moduli in $LiAlO_2$

Fabian Jachmann, M. Pattabiraman,[a] and Carsten Hucho[b]
Paul-Drude-Institut für Festkörperelektronik, Hausvogteiplatz 5-7, 10117 Berlin, Germany

(Received 28 April 2005; accepted 17 August 2005; published online 3 October 2005)

The precise determination of elastic constants of γ-$LiAlO_2$ has recently become important, as this material is being used as a substrate for intensely studied acousto-optical device structures and no values for the elastic moduli have been published to date. The precision of experimentally determined elastic constants hinges significantly on considering the influence of the acoustic transducer on the sound propagation in the system. Therefore, the influence of the transducer is discussed and an approach for corrections is presented. The compressional elastic constants C_{11} and C_{33} and the shear constants C_{12} and C_{13} of γ-$LiAlO_2$ are determined with an acoustic pulse-echo technique and with sampled-continuous-wave spectroscopy. © *2005 American Institute of Physics*.
[DOI: 10.1063/1.2061889]

I. INTRODUCTION

An increasing interest in group-III nitrides due to their technically important optical and in some cases acoustoelectrical properties has stimulated the search for optimum substrate materials. AlN and GaN layers, for example, are widely investigated because of their strong electromechanical coupling, which implies interesting device applications. Standard substrates such as Al_2O_2(0001) and SiC(0001), however, have strong drawbacks as the AlN and GaN films are oriented with their electric polarization axis out of plane. This leads to large spontaneous and induced electric fields which quench photoluminescence in GaN–(Al,Ga)N heterostructures and therefore counteract one of the most interesting properties for device fabrication. In contrast, *M*-plane GaN does not exhibit spontaneous electric polarization—it is nonpolar. This orientation was shown to grow well on tetragonal γ-$LiAlO_2$.[1] In addition, vanishing strain components along piezoactive axes lead to vanishing piezopolarization in strained layers.

While this work was stimulated by the need for precisely determined elastic constants of γ-$LiAlO_2$ for the design of acousto-optical device structures, their experimental determination is of more general interest since no elastic constants of γ-$LiAlO_2$ have been published to date.

II. EXPERIMENT

We investigate a single crystal of $LiAlO_2$ (Crystal-Tec) which was cut along the principal axes. The optically smooth surfaces of the cube with dimensions of $7\times7\times7$ mm^3 were covered with a layer of 5 nm CrNi and 150 nm Au to serve as temperature-independent ground contact for the overtone-polished acoustic quartz transducer (base frequency of 5 MHz). Four out of six independent elastic moduli of this tetragonal material can be determined using this sample. For the determination of $C_{11}(=C_{22})$ and C_{33} an *x*-cut quartz transducer was bonded to the sample with a liquid polymer (Thiokol LP32). For C_{12} and $C_{13}(=C_{23})$ an AC-cut quartz transducer was employed to excite transversely polarized acoustic waves. The sound-path length was determined to an accuracy of 15 μm.

The sound velocities were determined by measuring the transit times from an acoustic echo pattern and by the sampled-continuous-wave technique. With sample length l and echo separation Δt the sound velocity is given as $v=2l/\Delta t$. The precision of the results from pulse-echo experiments is limited by a number of factors. First of all there is a technical difficulty to define clear starting points for subsequent echoes as the echo shape deteriorates with time. Furthermore, the velocity measurement is only accurate if the influence of the transducer on the sound path can be ignored. This is generally not the case. The reflection point of the echo can be envisioned as being displaced into the transducer depending on the acoustic impedances of sample and transducer. Ignoring the influence of the transducer leads to underestimating the apparent sound-path length and, therefore, to an underestimated sound velocity and elastic modulus. Uncorrected pulse-echo experiments can, however, serve as a first approximation for determination of the elastic moduli[2] and an indication of the elastic anisotropy. The need for corrections due to phase shift upon reflection[3] and diffraction effects during stress pulse propagation[4] is known and analyzed for quite some time. Sophisticated technical modifications were employed to correct these effects.[5,6]

Sampled-continuous-wave (SCW) experiments, on the other hand, allow a very precise determination of acoustic resonances (which translate into sound velocities) but the influence of the transducer also has to be taken into account. The principle of operation of the SCW experiment is depicted in Fig. 1. In the SCW experiments described here a 50 μs pulse was applied to the transducer by a gated amplifier (Ritec GA2500) and the exponential "ring down" of the acoustic response was monitored by the same transducer after switching off the pulse. The envelope of the exponentially decaying signal determines the attenuation. The resonance frequency of the transducer-sample system was extracted with a resolution of less than 10 ppm from a fast fourier

[a]Mailing address: Materials Science Division, Indira Gandhi Centre for Atomic Research, Kalpakkam 603 102, India.
[b]Electronic mail: hucho@pdi-berlin.de

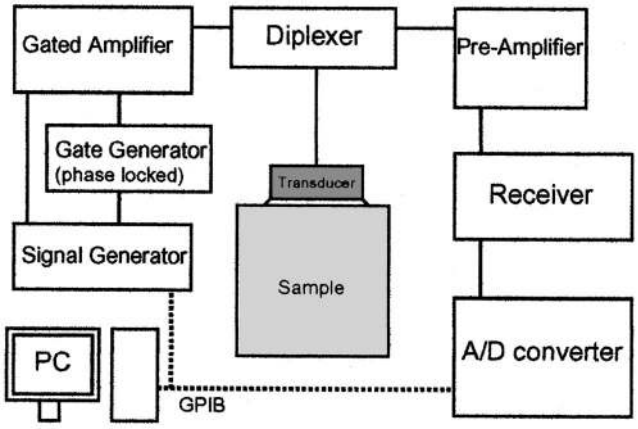

FIG. 1. Principle of operation of the sampled-continuous-wave setup. A high-power rf electromagnetic pulse from the amplifier excites a strain pulse in the transducer. The pulse length is chosen to be much longer than the travel time of a short acoustic pulse. After switching off the pulse, the acoustic ring down of the sample is detected by the same transducer, amplified, digitized, and finally analyzed. A fourier transform of the signal gives the frequency spectrum of the acoustic response. Here, the resonance frequency, attenuation, and amplitude can be extracted. The resonance frequency is fed back to the frequency source in order to warrant optimal matching of excitation and resonance frequencies.

transform (FFT) of the signal. The absolute value of the phase velocity is determined by recording the frequency-dependent amplitude of the exponentially decaying acoustic response—as shown in Fig. 2 for the compressional mode propagating along the crystallographic c axis. Clear amplitude maxima mark the acoustic resonances of the transducer-sample system. The amplitude increases for frequencies close to the resonance of the transducer and amplitude oscillations due to the interference with transducer modes become visible. Far away from the transducer resonance the sensitivity is greatly reduced and the determination of peak position becomes less accurate. The appearance of an additional peak structure is possibly attributable to a nonvanishing acoustoelectric coupling in some crystal axes as determined in Ref. 2.

If the influence of the transducer is ignored, a separation of resonances by Δf of a sample with length l_S is related to the sound velocity by the simple expression

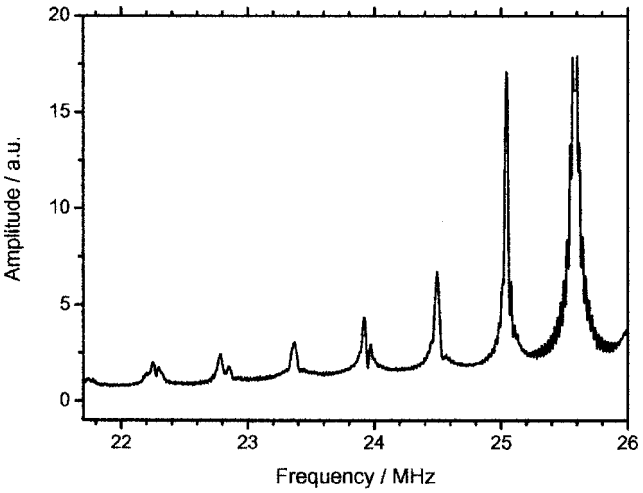

FIG. 2. Frequency-dependent amplitude of the acoustic response of $LiAlO_2$ for longitudinal sound propagating along the crystallographic c axis (C_{33}).

$$v_s = 2l_S\Delta f. \tag{1}$$

With the mass density ρ the elastic moduli are given by

$$C = \rho v_s^2. \tag{2}$$

Tetragonal γ-$LiAlO_2$ has six independent elastic moduli, four of which (two compressional modes: $C_{11}=C_{22}$ and C_{33} and two shear modes: C_{12} and C_{13}) are accessible using the crystal described above. The orientation of the crystal was checked and labeled using Raman scattering. The c axis of γ-$LiAlO_2$ is identified as the direction in which the Raman spectra with polarization along the two perpendicular crystal axes are indistinguishable.[2]

III. RESONANCE IN COMPOUND SYSTEMS

In all the experiments performed during this work ultrasound is applied and detected by a quartz transducer which is bonded to the sample surface. Therefore resonance measurements which correspond to measurements of the phase velocity always reflect the acoustic properties of two coupled subsystems having different sound velocities and attenuation constants. A correction of this impedance matching effect corresponds to a correction of the apparent sample length since the acoustic wave leaks into the transducer if the acoustic impedances are not perfectly *mismatched*. (This is, of course, never the case. Even if no transducer is employed, the acoustic radiation into the surrounding gas and the corresponding mass loading influences the resonances of the system albeit ever so slightly.[7]) Hence, the resonances reflect the properties of the coupled (transducer-sample) system comprising the sample with mass density ρ_S and the transducer with thickness l_T and mass density ρ_T. Detailed calculations by Bolef and Menes[8] and Miller and Bolef[9] lead to expressions which after some assumptions can be simplified to a modified sample length,

$$v = 2l_S(1+\delta)\Delta f \tag{3}$$

with

$$\delta = \frac{l_T\rho_T}{l_S\rho_S}. \tag{4}$$

This correction term was calculated assuming a large ratio of sample length to transducer thickness, while taking the attenuation in both, the sample and transducer, as negligibly small. In our measurements the damping of the sample is high compared to quartz and the length is sometimes of the same order as the transducer length. For this reason a more accurate calculation is needed. We employ a numerical solution that is not constrained by those assumptions to determine the sound velocity. In Ref. 9 it is shown that a summation of the propagating waves leads to the complex amplitude,

$$\tilde{A} = \exp(i\omega t)\frac{\exp(\Phi_1 2l_1)[\exp(\Phi_2 2l_2)+r]}{[\exp(\Phi_1 2l_1)-r][\exp(\Phi_2 2l_2)+r]-T^2}. \tag{5}$$

$\Phi_i=\alpha_i+ik_i$ describes the propagation of the wave in the medium with α_i being the attenuation constant and $k_i=2\pi f/v_i$ the wave vector, where f is the frequency and v_i is the phase

velocity. The acoustic impedance of a medium is given by $Z_i=\rho_i v_i$. In our case we identify the sample with $i=1$ and the transducer with $i=2$. Reflection and transmission coefficients are given as

$$r_{1\to 2}=(Z_1-Z_2)/(Z_1+Z_2), \tag{6}$$

$$T_{1\to 2}=2Z_1/(Z_1+Z_2). \tag{7}$$

Here, $r=r_{1\to 2}=-r_{2\to 1}$ and $T^2=T_{1\to 2}T_{2\to 1}$. The physically relevant real part A of the complex amplitude (5) can be separated into two terms:

$$A=A_I\cos\omega t+A_{II}\sin\omega t. \tag{8}$$

A_I is in phase with the driving oscillator and A_{II} is 90° phase shifted. Since we are interested in the resonance frequencies only (which correspond to a maximum in $A^2=A_I^2+A_{II}^2$) we can neglect A_{II} as it becomes zero for resonant conditions. The rather bulky expression for A_I is given in Ref. 9. At this point Miller and Bolef assume vanishing attenuation in the transducer and sample as well as a small transducer length compared to the length of the sample. They arrive at the widely used equation (3).

In contrast, the only approximation employed here is to neglect the attenuation of the transducer ($\alpha_2=0$). In order to find the resonance frequencies, the first derivative of A_I with respect to v_1 is calculated and set to zero. Since the denominator of the resulting expression remains finite for all values of v_S, it is sufficient to find the values of v_S for which the nominator vanishes. Some algebra leads to the condition for resonance,

$$\begin{aligned}0=&\sinh(\alpha_1 2l_1)[k_1l_1(Z_1^2+Z_2^2)+k_1l_1(Z_1^2-Z_2^2)\cos(2l_2k_2)\\&+Z_1Z_2\sin(2l_2k_2)]\cdot[2(Z_1^2-Z_2^2)\sin(2l_1k_1)\\&+(Z_1-Z_2)^2\sin(2l_1k_1-2l_2k_2)\\&+(Z_1+Z_2)^2\sin(2l_1k1+2l_2k_2)].\end{aligned} \tag{9}$$

For clarity we symbolize this expression by $\sinh(A)[B]\cdot[C]$ The attenuation of the sample is now only present in the prefactor $\sinh(A)$. Since the resonance condition has to hold for all values of $\alpha_1>0$ [corresponding to $\sinh(A)>0$] the position of the amplitude maxima of the whole system is sufficiently defined by the α-independent part of Eq. (9) becoming zero, i.e., $[B]\cdot[C]\equiv 0$. Therefore we can conclude that in A_I *both* attenuation constants can be set to zero. Maxima of A_I are found, where the denominator of A_I in Ref. 9 vanishes. Simplification leads to the condition for resonance,

$$0=z_1\cos(k_2l_2)\sin(k_1l_1)+z_2\cos(k_1l_1)\sin(k_2l_2). \tag{10}$$

In order to determine the sound velocity in our sample we therefore evaluate those k- (and thereby velocity-) dependent frequency spectra numerically. As the result is a set of solutions, we approach the correct result by introducing the velocity measured from pulse-echo experiments as input and calculate the resulting frequency-dependent amplitudes (the frequency spectrum) for a range of velocities around this first approximation. These spectra are compared to the experimental data and optimized for maximum overlap by adjusting the velocity v_1. The calculated spectrum with minimum deviation from the experimental results yields the final result for the phase velocity in the sample. In the following paragraph we compare the results of pulse-echo experiments, the SCW experiments evaluated by Eq. (3) and SCW experiments with the refined correction described above.

TABLE I. The elastic moduli of γ-$LiAlO_2$ as determined by pulse-echo (labeled "pulse") and SCW experiments. SCW_δ denotes results with the "conventional" correction of Eq. (3), SCW_{num} are the results as obtained with the refined numerical correction described above. The errors ΔC reflect a summation of errors in determining the sample length, mass density, and pulse separation or resonance frequency. The systematic error of underestimating the "true" sound-path length is visible in the trend from the uncorrected pulse results over conventionally corrected SCW experiments to the improved correction of SCW_{num}.

Method	C_{11} (10^{11} N/m^2)	C_{33} (10^{11} N/m^2)	C_{12} (10^{11} N/m^2)	C_{13} (10^{11} N/m^2)	ΔC
Pulse	148.49	178.42	68.08	68.73	2.5%
SCW_δ	152.19	184.69	72.13	71.72	2%
SCW_{num}	161.84	194.74	74.10	73.87	2%

IV. RESULTS AND DISCUSSION

The results of the sound velocity measurements are compiled in Table I. Velocities are converted to elastic moduli using Eq. (2) and a mass density of 2.63×10^3 kg/m^3. The influence of the transducer on the apparent velocity is clearly visible, with the uncertainty in pulse-echo measurements being largest due to difficulties in determining the pulse positions exactly (about 2% for the echo separation Δt). All data presented in Table I are higher than the uncorrected data from a combination of pulse-echo and SCW experiments reported earlier.[2] The largest error in the SCW results is due to the general uncertainty in selecting the correct v_S out of the set of possible solutions for resonance. If the solutions are too close (i.e., the sample is very large compared to the acoustic wavelength), starting from the velocity as determined by pulse-echo technique may lead to a local minimum in the solution, which can be several wavelengths off the "true" result. We have therefore determined the sound velocity for a wide range of frequencies, with the lowest frequencies allowing for the determination of the "correct" minimum and the highest frequencies then yielding the highest resolution with this input.

The errors ΔC given in the table are the statistical errors due to a limited resolution in the determination of the sound-path length and the mass density, and not the systematic error due to neglecting the influence of the transducer. The systematic error is largest for the uncorrected pulse-echo measurements and smallest for the SCW_{num} evaluation. The error in the determination of the path lengths can be estimated to be about 15 μm, corresponding to 1.1% of the total sound path. The overall resolution of the numerical fit to the experimental results is determined by measuring the nominally identical C_{13} and C_{23} and by evaluating the scattering of the data. This error is of the order of 1%.

V. CONCLUSION

The influence of a transducer on the experimental determination of the elastic moduli of a solid sample was discussed and an approach for corrections was presented. Using an acoustic sampled-continuous-wave experiment to determine the acoustic resonances of a γ-$LiAlO_2$ single crystal allowed for the determination of the compressional elastic constants C_{11} and C_{33} and the shear constants C_{12} and C_{13}. It was shown that uncorrected SCW and pulse-echo experiments seriously underestimate the sound velocity.

[1] P. Waltereit, O. Brandt, A. Trampert, H. T. Grahn, J. Menninger, M. Ramsteiner, M. Reiche, and K. H. Ploog, Nature (London) **406**, 865 (2000).
[2] Y. Takagaki, C. Hucho, E. Wiebicke, Y. J. Sun, O. Brandt, M. Ramsteiner, and K. H. Ploog, Phys. Rev. B **69**, 115317 (2004).
[3] R. C. Williamson, J. Acoust. Soc. Am. **45**, 1251 (1969).
[4] M. R. Layton, E. F. Carome, H. D. Hary, and J. A. Bucaro, J. Acoust. Soc. Am. **84**, 250 (1978).
[5] T. J. Kim and W. Grill, Ultrasonics **36**, 233 (1998).
[6] M. J. Lang, M. Duarte-Dominguez, and W. Arnold, Rev. Sci. Instrum. **71**, 3470 (2000).
[7] H. Zhang *et al.*, J. Acoust. Soc. Am. **103**, 2385 (1998).
[8] D. I. Bolef and M. Menes, J. Appl. Phys. **31**, 1010 (1960).
[9] J. G. Miller and D. I. Bolef, J. Appl. Phys. **39**, 4589 (1968).